Differential coding of humoral stimuli by timing and amplitude of intracellular calcium spike trains

M. Kropp, F. Gabbiani and K. Prank

Abstract: The ubiquitous Ca^{2+}-phosphoinositide pathway transduces extracellular signals to cellular effectors. Using a mathematical model, we simulated intracellular Ca^{2+} fluctuations in hepatocytes upon humoral stimulation. We estimated the information encoded about random humoral stimuli in these Ca^{2+}–spike trains using an information-theoretic approach based on stimulus estimation methods. We demonstrate accurate transfer of information about random humoral signals with low temporal cutoff frequencies. In contrast, our results suggest that high-frequency stimuli are poorly transduced by the transmembrane machinery. We found that humoral signals are encoded in both the timing and amplitude of intracellular Ca^{2+} spikes. The information transmitted per spike is similar to that of sensory neuronal systems, in spite of several orders of magnitude difference in firing rate.

1 Introduction

The Ca^{2+}-phosphoinositide signalling pathway plays a major role in transmembrane and intracellular signalling in a number of different cell types [1]. Upon binding to plasma membrane receptors, hormones, growth factors and neurotransmitters initiate the activation of G-proteins and phospholipase C (PLC) and the subsequent formation of diacylglycerol (DAG) and inositol(1,4,5)-trisphosphate ($InsP_3$), which triggers the generation of repetitive spikes of the intracellular calcium concentration ($[Ca^{2+}]_i$). Both amplitude modulation (AM) and frequency modulation (FM) are used to regulate cellular processes differentially [2]. The FM mode of $[Ca^{2+}]_i$-signalling is known to stimulate secretory processes [3], glycogen metabolism in hepatocytes [4, 5], differentiation in nerve cells [6, 7] and differential gene transcription [8]. In addition, experimental data from B lymphocytes link the AM mode and the duration, but not the frequency, of $[Ca^{2+}]_i$ spikes to differential gene activation [9].

It has been demonstrated in single hepatocytes that constant levels of extracellular humoral agonists are encoded in the frequency of $[Ca^{2+}]_i$ spikes following α_1-adrenergic stimulation [4]. However, most extracellular agonists, such as hormones, neurotransmitters and cytokines, are not released in a constant, but rather in a pulsatile, fashion [10]. Based on this fact, Schöfl *et al.* [5] performed experiments in single primary rat hepatocytes, demonstrating the transmembrane transduction of pulsatile α_1-adrenergic stimuli into repetitive $[Ca^{2+}]_i$ spikes. This work showed that, not only the frequency, but also the amplitude of $[Ca^{2+}]_i$ spikes can be altered by the pattern of stimulation. A striking analogy to neuronal signalling was observed as distinct types of entrainment regime were shown to exist between the extracellular α_1-adrenergic stimulus and the intracellular $[Ca^{2+}]_i$ spikes. Based on these experimental findings, Chay *et al.* [11] developed a mathematical model for G-protein coupled, receptor-controlled $[Ca^{2+}]_i$ spiking that explained most of the experimentally discovered features.

We used this model to estimate the information conveyed about external humoral signals to intracellular effectors by the Ca^{2+}-phosphoinositide signalling pathway. More specifically, we assessed whether the FM, the AM and the timing variability of individual spikes have an impact on the coding capabilities of the Ca^{2+} signal. The basic idea behind our approach was to estimate a given random extracellular humoral stimulus by convolving the $[Ca^{2+}]_i$-spike train with a temporal filter, as shown schematically in Fig. 1. This allows us to compute the fidelity of transduction and to estimate the rate of information transmission. Our results are compared with those obtained in the context of neuronal signalling.

2 Results

We used two different measures to quantify the fidelity of transmembrane signal transduction (Section 4). The first one is called the coding fraction and is a relative measure of the quality with which the humoral stimulus can be estimated from intracellular $[Ca^{2+}]_i$ signals. The coding fraction takes a value of one (100%) when the stimulus can be perfectly reconstructed from the intracellular $[Ca^{2+}]_i$-spike train, whereas a value of zero means that reconstruction of the random humoral stimulus is at chance level. A second, absolute measure is given by the information rate or mutual information (in bits s^{-1} or bits per spike) transmitted between the extracellular humoral stimulus and the intracellular $[Ca^{2+}]_i$-spike train.

2.1 Higher coding capacity for more regular stimuli

By varying the cutoff frequency of the random humoral stimuli, we found that the coding capability of $[Ca^{2+}]_i$

IEE Proceedings online no. 20050040

doi:10.1049/ip-syb:20050040

Paper first received 30th June 2005

M. Kropp is with the Hannover Medical School, Hannover D-30623, Germany

F. Gabbiani is with the Department of Neuroscience, Baylor College of Medicine, Houston, Texas 77030, USA

K. Prank is with the Hannover Medical School, Hannover D-30623, Germany and NRW Graduate School in Bioinformatics & Genome Research, Bielefeld University, Bielefeld D-33615, Germany

E-mail: klaus.prank@cebitec.uni-bielefeld.de

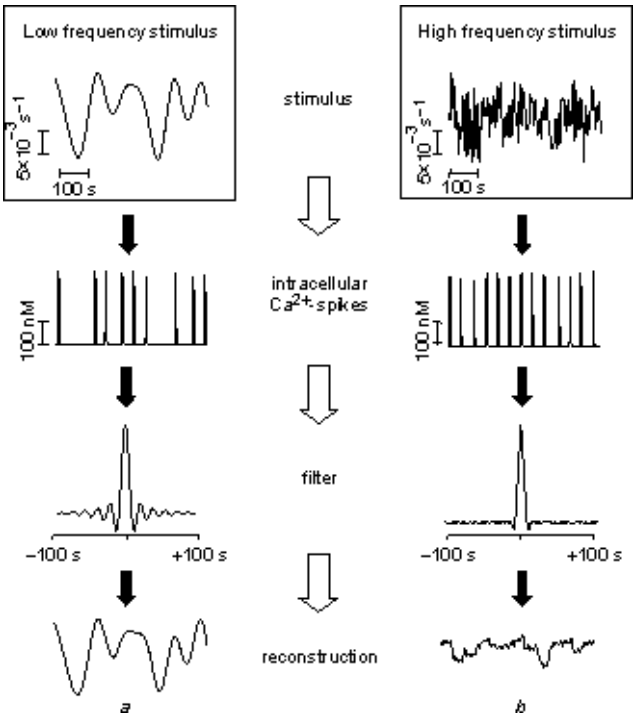

Fig. 1 *Low-frequency stimuli have higher coding capability*

a Reconstruction of low-frequency stimulus (cutoff frequency 10 mHz) is in good agreement with original stimulus and is associated with distinct modulation of ISIs in $[Ca^{2+}]_i$-spike train

b In contrast, reconstruction of high-frequency stimulus (cutoff frequency 100 mHz) is rather poor. This is in agreement with lack of major variations in ISIs of $[Ca^{2+}]_i$-spike train. Low-frequency stimulus yielded reconstruction filter with major positive and negative filter coefficients in both temporal directions, whereas filter generated from high-frequency stimulus has only one major peak centred around zero. Thus variation of ISIs for low-frequency stimulus allows capture of most of dynamics in reconstructed stimulus. In case of high-frequency stimulus, $[Ca^{2+}]_i$-spike train has almost identical ISIs just allowing for reconstruction of moving average of original stimulus

spikes is maximised for low-frequency stimuli. Both the coding fraction (Fig. 2) and the information rate (Fig. 3) increased with decreasing cutoff frequencies (and thus more regular stimuli), taking their maximum values at cutoff frequencies below 20 mHz. The maximum coding fraction was found at a stimulus cutoff frequency of 4 mHz and a $[Ca^{2+}]_i$-spike frequency of 29 mHz. In general, stimulus reconstructions with a coding fraction higher than 70% were achieved for stimuli with cutoff frequencies below 10 mHz and $[Ca^{2+}]_i$-spiking frequencies between 20 and 30 mHz. In contrast, generating significant information rates strongly depended on the $[Ca^{2+}]_i$-spike frequency exceeding a threshold of 25 mHz and the stimulus cutoff frequency being above 10 mHz. The information rate took its maximum (0.037 bits s^{-1}) at a stimulus cutoff frequency of 13 mHz. This maximum occurred at a $[Ca^{2+}]_i$-spike frequency of 30 mHz, corresponding to 1.2 bits per spike. Thus the maximum information rates occurred at a higher cutoff frequency than the maximum coding fractions and increased very fast for low-frequency stimuli. This is presumably owing to the rapid increase in information content in the stimulus with frequency at low cutoff frequencies.

2.2 AMs increase information rates and coding fractions

Two variables of the Ca^{2+} spike trains could convey information about the humoral stimulus: the interspike intervals (ISIs) and the amplitude of individual spikes (Fig. 1). To tease apart the contribution made by these two factors, we estimated the humoral stimuli using exclusively the ISI information by clamping the amplitude of Ca^{2+} spikes to a fixed value (400 nM).

The reconstruction quality was substantially higher when both ISI and amplitude information were used, compared with using only ISI information. The maximum of the coding fraction was reduced from 94% (ISI and amplitude information) to 75% (ISI information only). Thus about 20%, or slightly less than one-third, of the information conveyed by spike timing is conveyed by spike amplitude. Similarly, the information rate significantly decreased when amplitude information was excluded from the $[Ca^{2+}]_i$ signal (Fig. 3*b*). The information rate was reduced from 0.037 bits s^{-1} (ISI and amplitude information) to 0.022 bits s^{-1} (ISI information only). The information rate is thus reduced by approximately one-third by clamping of the $[Ca^{2+}]_i$-spike amplitudes.

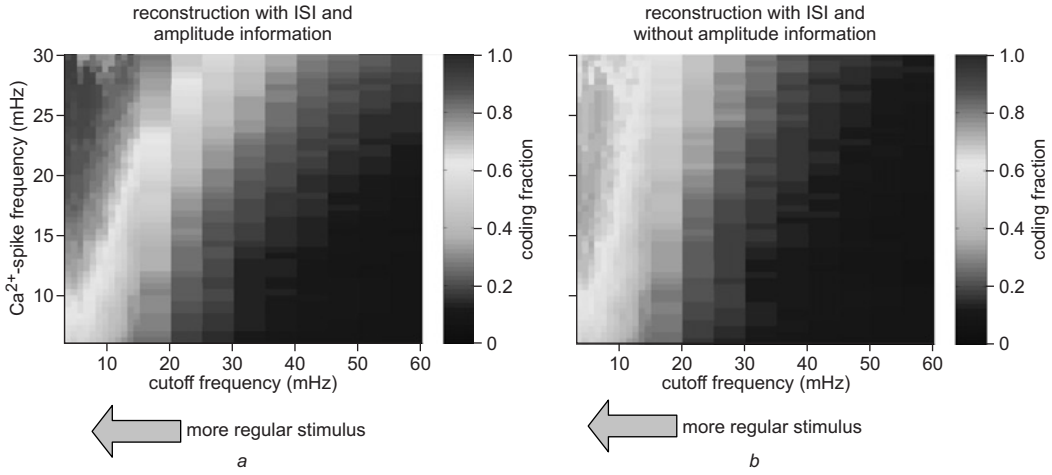

Fig. 2 *AMs increases information encoded by $[Ca^{2+}]_i$ signal*

a Up to 94% of fluctuations in stimuli can be encoded by $[Ca^{2+}]_i$-spike trains using ISI and amplitude information. Maximum was found at cutoff frequency of stimulus of 4 mHz and $[Ca^{2+}]_i$-spike frequency of 29 mHz

b This is reduced to maximum of 75% for $[Ca^{2+}]_i$-spike trains without amplitude information. To differentiate information encoded in timing of ISIs and amplitude of $[Ca^{2+}]_i$ signal, we clamped amplitude to fixed value. We found area of high coding capacity above coding fraction of 70% at cutoff frequencies of stimulus below 10 mHz and at $[Ca^{2+}]_i$-spike frequencies between 20 mHz and 30 mHz

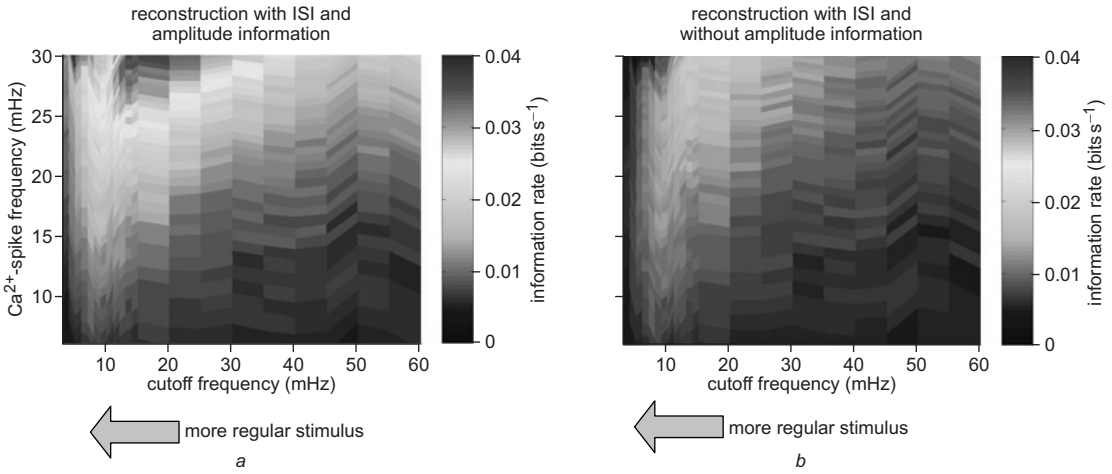

Fig. 3 *Absolute information rate increases with $[Ca^{2+}]_i$-spike frequency*

a High values of information rate above 0.035 bits s^{-1} are found at cutoff frequencies of stimulus between 10 and 25 mHz and for $[Ca^{2+}]_i$-spike frequencies above 25 mHz. Maximum of 0.037 bits s^{-1} for information rate was found at cutoff frequency of 13 mHz and $[Ca^{2+}]_i$-spike frequency of 30 mHz. This corresponds to 1.2 bits per spike. Maximum information rate occurred at higher cutoff frequency than for coding fraction and increased rapidly for low-frequency stimuli because of their low information content. In contrast to coding fraction, maximum information rates are obtained in tighter region and strongly depend on $[Ca^{2+}]_i$ -spike frequency and stimulus cutoff frequency exceeding 25 and 10 mHz, respectively

b Information rate decreased to 0.022 bits s^{-1} without amplitude information in $[Ca^{2+}]_i$ signal. This corresponds to one-third decrease when amplitude of $[Ca^{2+}]_i$ signal was clamped to fixed value

2.3 Information transfer requires ISI variability

As may be expected from Fig. 1, the variability of ISIs played an important role in the coding of dynamic stimulus information. To quantify the role played by ISI variability, we explored the dependence of the coding fraction and information rate on the coefficient of variation (CV) of the ISI distribution (equal to the ISI standard deviation divided by its mean). We generated $[Ca^{2+}]_i$-spike trains with increasing CVs by varying the mean amplitude of the stimulus with a fixed frequency content. This manipulation left the mean $[Ca^{2+}]_i$-spike train firing rate unchanged. A maximum of the coding fraction of 94% was found at a CV of 0.3 (Fig. 4*a*). When only ISI information was taken into account, the coding fraction took a lower value of 72% at the same CV. Figure 4*b* illustrates the convex shape of the information rate dependent on the CV, with a maximum at a CV of 0.24, irrespective of whether amplitude information is taken into account or not. The maximum information rates were 0.034 and 0.019 bits s^{-1} for $[Ca^{2+}]_i$-spike trains, with and without amplitude information, respectively. Thus Fig. 4 clearly demonstrates the decrease in coding capacity for more regular $[Ca^{2+}]_i$-spike trains both in terms of coding fraction and information rate.

3 Discussion

In this study, we present a novel application of stimulus estimation methods to Ca^{2+} signalling that was inspired by their recent success in analysing the information content of neuronal spike trains. These methods should be of broad interest, as they can be applied to the analysis of other downstream events, such as the activation of kinases or transcription factors by Ca^{2+}, and for estimating the flow of information between intracellular signalling pathways (cross-talk) as well as intercellular communication. Because the mathematical model used for simulating transmembrane signal transduction is based on coupled non-linear differential equations, it is not *a priori* clear that linear estimation methods will yield useful insight. However, we were able to reconstruct the stimulus dynamics nearly optimally by means of such linear filters, as we find values for the coding fraction up to 94%. This is in agreement with stimulus reconstruction approaches for sensory neuronal systems, where non-linearities associated with the spike generation mechanism and those determining the gain of neuronal responses are known not to hamper reconstructions [12, 13]. Based on the present simulations and on experimental results in sensory neuronal preparations, we thus also expect this method to be applicable to the study of transmembrane biochemical signal transduction in experimental preparations. Stimulus reconstruction techniques are expected to be useful experimentally, provided that both the Ca^{2+} and stimulus fluctuations lie in an appropriate frequency range and provided that both signals can be recorded over sufficiently long periods of time to allow for the computation of the reconstruction filter (in the order of a few thousand Ca^{2+} spikes).

The analysis presented here allowed us to explore the effect of temporal stimulus bandwidth on the accuracy of the transmembrane coding/decoding machinery. We found that high-frequency stimuli cannot be coded in $[Ca^{2+}]_i$-spike trains. Physiologically, α_1-receptors are activated by norepinephrine, which is released either from nerve endings in the liver or into the systemic blood circulation from the adrenal gland. The time scale of pulsatile norepinephrine release from the nerve endings, as well as systemic release, is in very good agreement with the mean period (between 1 and 6 min) optimally encoded in our simulations. Stimuli with a higher frequency were thus filtered out of the $[Ca^{2+}]_i$-spike train by the signal transduction machinery. To encode such stimulus fluctuations efficiently also requires a minimum number of $[Ca^{2+}]_i$ spikes, i.e. a minimum $[Ca^{2+}]_i$-spike frequency. When the $[Ca^{2+}]_i$-spike frequency is too low, the $[Ca^{2+}]_i$-signal is not capable of representing even low-frequency stimuli. Although most of the stimulus information is encoded in the interspike interval, there is an additional significant proportion encoded in the amplitude. Both maxima for the coding fraction were found at physiologically relevant values for the cutoff frequency of the stimulus [14] as well as the $[Ca^{2+}]_i$-spike frequency [4, 5]. The $[Ca^{2+}]_i$-spike frequencies found in this investigation are in good agreement with experimental

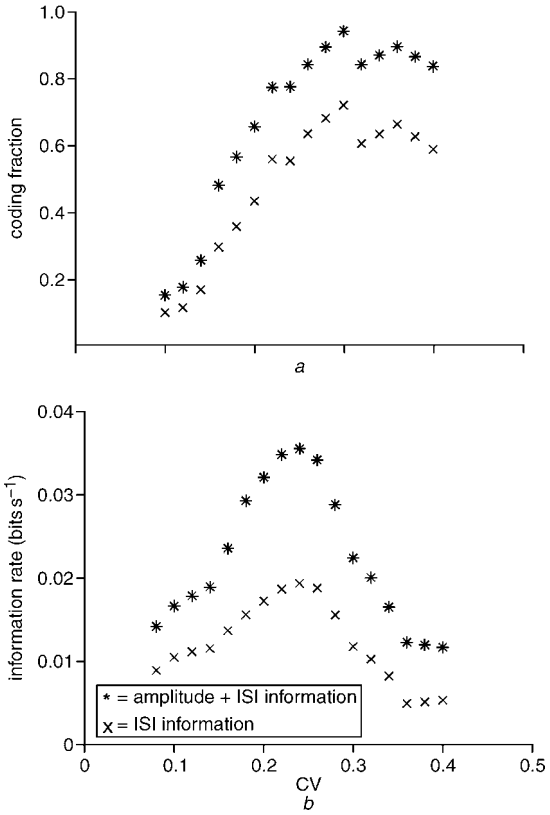

Fig. 4 *Significant coding requires ISI variability*

a Maximum of coding fraction of 94% was found at CV of 0.3. This was reduced to 72% for $[Ca^{2+}]_i$-spike train containing ISI information only

b Maximum of information rate was reached at CV of 0.24. For both coding fraction and information rate, low CVs, i.e. restricted variations in ISIs, lead to small values indicating low coding capacity. Specific value of spike timing variability around CV = 0.3 is required to obtain optimum coding capacity

data obtained from Schöfl *et al.* in hepatocytes upon α_1-adrenergic stimulation, where a $[Ca^{2+}]_i$-spike frequency between one every 30 s to one every 3 min was observed [4, 5].

We found an analogous behaviour for the information rate in the same operational range of $[Ca^{2+}]_i$-spike frequencies and stimulus cutoff frequencies. Regular stimuli have small information content: in the extreme case, a static stimulus would yield a $[Ca^{2+}]_i$-spike train with constant ISIs and vanishing information content. Our data indicate that the Ca^{2+}-phosphoinositide signalling pathway works optimally between such complete regularity and the irregular behaviour found at higher stimulus frequencies. We also found a similar dependence of the coding fraction and information rate on the regularity of $[Ca^{2+}]_i$-spike trains. At a fixed $[Ca^{2+}]_i$-spike frequency, $[Ca^{2+}]_i$-spike trains thus need some amount of variation in the timing of $[Ca^{2+}]_i$ spikes to encode the dynamics of the stimulus.

Although the information rates computed here are three or four orders of magnitude lower than those obtained in sensory neuronal systems, the information carried per $[Ca^{2+}]_i$ spike is of the same order as for neuronal spikes (action potentials [15]). Thus there might be a general principle of information coding in electrically excitable systems, such as the nervous system, and in biochemical communication, as exemplified by $[Ca^{2+}]_i$ signalling. In our system, however, this rate is achieved by encoding the signal both with ISIs and amplitudes of the Ca^{2+}-spike trains. In contrast, the electrical spikes of neurons are usually stereotyped in amplitude, and coding occurs only through ISI variations.

Our results suggest that a cell can use Ca^{2+} signals to regulate different downstream processes by varying both their amplitude and frequency. However, the versatility of $[Ca^{2+}]_i$ signalling and its information capacity are increased even further by the use of precise spike timing for encoding information.

4 Methods

We used the model proposed by Chay *et al.*, which is described in detail elsewhere [11]. Each $[Ca^{2+}]_i$-spike train $x(t)$ was simulated for 40 000 s using source code written for MATLAB*. The system of coupled, non-linear ordinary differential equations was integrated using a modified Rosenbrock formula stiff solver with variable integration time step. The stimulus $s(t) + s_{mean}$, which corresponds to k_g, the rate of activation of the G-protein in the model of Chay *et al.*, was generated by the low-pass filtering of uncorrelated, zero-mean, Gaussian white noise and then the rescaling of this signal to the interval [0 s^{-1}; 0.06 s^{-1}]. We varied the maximum stimulus amplitude between 0.015 and 0.060 s^{-1} to investigate the impact of increasing mean Ca^{2+}-spike frequency on the coding performance. Filtering was performed in the frequency domain by setting Fourier coefficients above the desired cutoff frequency f_c, of the stimulus $s(t)$ to zero. The cutoff frequency f_c ranged from 3 to 60 mHz.

To estimate the information about the time-varying hormonal concentration encoded in $[Ca^{2+}]_i$-spike trains in our simulation, we used the following stimulus reconstruction algorithm [12, 16, 17]. Let

$$x(t) = [Ca^{2+}](t) - \langle [Ca^{2+}] \rangle \tag{1}$$

be the $[Ca^{2+}]_i$-spike train with the mean calcium concentration subtracted. This spike train contains amplitude and timing information. We derived from (1) a $[Ca^{2+}]_i$-spike train containing only timing (ISI) information by defining a spike as an event that exceeded a threshold $[Ca^{2+}](t)$ of 400 nm and noted the time t_i of peak calcium concentration. An equivalent spike train was obtained by placing a Dirac delta function at each occurrence time t_i,

$$x(t) = \sum_i \delta(t - t_i) - x_0 \tag{2}$$

and by subtracting the mean value x_0 (i.e. the mean spike frequency).

A linear estimate $s_{est}(t)$ of the stimulus $s(t)$, given the spike train, is calculated by convolving the $[Ca^{2+}]_i$-spike train with a filter $h(t)$

$$s_{est}(t) = \int_0^T dt' h(t - t') x(t') \tag{3}$$

The filter $h(t)$ was chosen to minimise the mean square error ε^2 between the stimulus and estimate

$$\varepsilon^2 = \frac{1}{T} \int_0^T dt [s(t) - s_{est}(t)]^2 \tag{4}$$

*MathWorks Inc., Natick, MA.

where the integration is over the duration of the simulation ($T = 40\,000$ s). Solving for the filter $h(t)$ leads to

$$h(t) = \int_{-f_c}^{f_c} \mathrm{d}f \, \frac{S_{sx}(-f)}{S_{xx}(f)} \mathrm{e}^{-i2\pi ft} \tag{5}$$

In (5), f_c is the cutoff frequency of the stimulus, $S_{sx}(f)$ represents the Fourier transform of the cross-correlation between the stimulus and the spike train, and $S_{xx}(f)$ represents the Fourier transform of the autocorrelation function of the $[Ca^{2+}]_i$-spike train. We define the cross-correlation between the stimulus $s(t)$ and the spike train $x(t)$ as

$$R_{sx}(\tau) = \frac{1}{T} \int_0^T \mathrm{d}t \, s(t)x(t+\tau) \tag{6}$$

and the autocorrelation function of the $[Ca^{2+}]_i$-spike train $x(t)$ as

$$R_{xx}(\tau) = \frac{1}{T} \int_0^T \mathrm{d}t \, x(t)x(t+\tau) \tag{7}$$

The filter $h(t)$, computed from (5), is not causal in general, in the sense that $h(t) \neq 0$ for $t > 0$, i.e. the occurrence of a spike can be used to predict the future temporal dynamics of the stimulus (this is, of course, only possible because of correlations in the stimulus and because of the response properties of the simulated cell). Causality is usually implemented by the introduction of a time delay into the reconstructions [12] or by the application of a causal Wiener–Kolmogorov filter [18]. If no correlations exist between the stimulus $s(t)$ and the spike train $x(t)$, (i.e. $S_{sx}(f) = 0$ for all frequencies f), the best linear estimate of the stimulus $s(t)$ is equal to the mean value $\langle s(t) \rangle = 0$. The maximum mean square error computed from (4) is then equal to the variance of the stimulus $\varepsilon^2 = \sigma_s^2$. Once the best linear estimate $s_{est}(t)$ is found, the 'noise' contaminating the reconstructions is defined as the difference between the estimated stimulus $s_{est}(t)$ and the original stimulus $s(t)$

$$n(t) = s_{est}(t) - s(t) \tag{8}$$

The mean square error in the reconstructions [19] is then given by

$$\varepsilon^2 = \int_{-f_c}^{f_c} \mathrm{d}f \, \frac{S_{ss}(f)}{SNR(f)} \tag{9}$$

where the signal-to-noise ratio (SNR) is defined as

$$SNR(f) = \frac{S_{ss}(f)}{S_{nn}(f)} \geq 1 \tag{10}$$

In (10), $S_{nn}(f)$ and $S_{ss}(f)$ are the power spectra of the noise and the stimulus, respectively. Thus the SNR $SNR(f)$ is a measure of the amount of signal power present at a given frequency relative to the noise contaminating the reconstructions. In the extreme case where the spike train is completely unrelated to the signal, $SNR(f) = 1$ for all frequencies; otherwise $SNR(f) > 1$.

The accuracy of the reconstruction and thus the information transmitted from the stimulus $s(t)$ to the spike train $x(t)$ is determined by the coding fraction, defined as

$$\gamma = 1 - \frac{\varepsilon}{\sigma} \tag{11}$$

where ε is the root mean square error (RMSE) between the actual stimulus $s(t)$ and the estimated stimulus $s_{est}(t)$, and σ is the standard deviation of the stimulus $s(t)$ [19]. Thus the coding fraction represents the percentage of temporal stimulus fluctuations encoded, in units of the stimulus standard deviation. The coding fraction takes a maximum value of 1 when the stimulus is perfectly estimated ($\varepsilon = 0$) and the minimum value of 0 if the stimulus estimation from the $[Ca^{2+}]_i$-spike train is at chance level ($\varepsilon = \sigma$) [17, 20]. The accuracy of encoding in different simulations can be compared on the basis of the coding fraction. Bialek and collaborators [12, 16] used a different measure, the mutual information transmitted by the reconstructions $s_{est}(t)$ about the stimulus $s(t)$. For a Gaussian white-noise stimulus, the ε-entropy or rate of distorsion function is defined as

$$I_\varepsilon = \frac{-f_c}{\log(2)} \log\left(\frac{\varepsilon}{\sigma}\right) \quad (\text{bits s}^{-1}) \tag{12}$$

and is an absolute lower bound for the equivalent rate of information transmission [19, 21]. In contrast to the estimation of the information rate, the metric used for the reconstruction is independent of Gaussian assumption. The rate of information transmitted per $[Ca^{2+}]_i$ spike is obtained by dividing I_ε by the mean $[Ca^{2+}]_i$-spike frequency λ

$$I_s = \frac{I_\varepsilon}{\lambda} \quad (\text{bits per spike}) \tag{13}$$

5 Acknowledgments

This work was supported by Deutsche Forschungsgemeinschaft under grant Pr 333/17-1 and the NRW Graduate School in Bioinformatics and Genome Research. F. Gabbiani was supported by an Alfred P. Sloan Research Fellowship.

6 References

1 Berridge, M.J., Bootman, M.D., and Roderick, H.L.: 'Calcium signalling: dynamics, homeostasis and remodelling', *Nat. Rev. Mol. Cell Biol.*, 2003, **4**, pp. 517–529
2 Berridge, M.J.: 'The AM and FM of calcium signalling', *Nature*, 1997, **386**, pp. 759–760
3 Rapp, P.E., and Berridge, M.J.: 'The control of transepithelial potential oscillations in the salivary gland of *Calliphora erythrocephala*', *J. Exp. Biol.*, 1981, **93**, pp. 119–132
4 Woods, N.M., Cuthbertson, K.S., and Cobbold, P.H.: 'Repetitive transient rises in cytoplasmic free calcium in hormone-stimulated hepatocytes', *Nature*, 1986, **319**, pp. 600–602
5 Schöfl, C., Brabant, G., Hesch, R.D., von zur Muhlen, A., Cobbold, P.H., and Cuthbertson, K.S.: 'Temporal patterns of alpha 1-receptor stimulation regulate amplitude and frequency of calcium transients', *Am. J. Physiol.*, 1993, **265**, pp. 1030–1036
6 Gomez, T.M., Robles, E., Poo, M., and Spitzer, N.C.: 'Filopodial calcium transients promote substrate-dependent growth cone turning', *Science*, 2001, **291**, pp. 1983–1987
7 Tang, F., Dent, E.W., and Kalil, K.: 'Spontaneous calcium transients in developing cortical neurons regulate axon outgrowth', *J. Neurosci.*, 2003, **23**, pp. 927–936
8 Dolmetsch, R.E., Xu, K., and Lewis, R.S.: 'Calcium oscillations increase the efficiency and specificity of gene expression', *Nature*, 1998, **392**, pp. 933–936
9 Dolmetsch, R.E., Lewis, R.S., Goodnow, C.C., and Healy, J.I.: 'Differential activation of transcription factors induced by Ca^{2+} response amplitude and duration', *Nature*, 1997, **386**, pp. 855–858
10 Brabant, G., Prank, K., and Schöfl, C.: 'Pulsatile patterns in hormone secretion', *Trends Endocrinol. Metab.*, 1992, **3**, pp. 183–190
11 Chay, T.R., Lee, Y.S., and Fan, Y.S.: 'Appearance of phase-locked Wenckebach-like rhythms, devil's staircase and universality in intracellular calcium spikes in non-excitable cell models', *J. Theor. Biol.*, 1995, **174**, pp. 21–44

12 Bialek, W., Rieke, F., de Ruyter van Steveninck, R.R., and Warland, D.: 'Reading a neural code', *Science*, 1991, **252**, pp. 1854–1857
13 Gabbiani, F., and Koch, C.: 'Principles of spike train analysis', in Koch, C., and Segev, I. (Eds.): 'Methods in neuronal modeling' (MIT Press, Cambridge, MA, 1998), pp. 313–360
14 Schöfl, C., Becker, C., Prank, K., Von Zur Mühlen, A., and Brabant, G.: 'Twenty-four-hour rhythms of plasma catecholamines and their relation to cardiovascular parameters in healthy young men', *Eur. J. Endocrinol.*, 1997, **137**, pp. 675–683
15 Bialek, W., and Rieke, F.: 'Reliability and information transmission in spiking neurons', *Trends. Neurosci.*, 1992, **15**, pp. 428–434
16 Rieke, F., Warland, D., and Bialek, W.: 'Coding efficiency and information rates in sensory neurons', *Europhys. Lett.*, 1993, **22**, pp. 151–156
17 Gabbiani, F.: 'Coding of time-varying signals in spike trains of linear and half-wave rectifying neurons', *Comp. Neural. Syst.*, 1996, **7**, pp. 61–85
18 Poor, H.V.: 'An introduction to signal detection and estimation' (Springer-Verlag, New York, 1994, 2nd edn.)
19 Wessel, R., Koch, C., and Gabbiani, F.: 'Coding of time-varying electric field amplitude modulations in a wave-type electric fish', *J. Neurophysiol.*, 1996, **75**, pp. 2280–2293
20 Gabbiani, F., and Koch, C.: 'Coding of time-varying signals in spike trains of integrate-and-fire neurons with random threshold', *Neural Comput.*, 1996, **8**, pp. 44–66
21 Shannon, C.E., and Weaver, W.: 'The mathematical theory of communication' (Illinois University Press, Urbana, IL, 1963)